Field-induced phase transitions in chiral smectic liquid crystals studied by the constant current method

H Dhaouadi†, R Zgueb, O Riahi, F Trabelsi, and T Othman

Département de physiqu, Faculté des Sciences de Tunis, Laboratoire de physique de la matière molle et de modélisation électromagnétique (LP3ME), Université Tunis Elmanar Campus universitaire 2092, *Tunis, Tunisia*

(Received 12 November 2015; revised manuscript received 7 January 2016; published online 5 April 2016)

In ferroelectric liquid crystals, phase transitions can be induced by an electric field. The current constant method allows these transition to be quickly localized and thus the (E,T) phase diagram of the studied product can be obtained. In this work, we make a slight modification to the measurement principles based on this method. This modification allows the characteristic parameters of ferroelectric liquid crystal to be quantitatively measured. The use of a current square signal highlights a phenomenon of ferroelectric hysteresis with remnant polarization at null field, which points out an effect of memory in this compound.

Keywords: chiral smectic liquid crystal, constant current method, ferroelectric polarization dielectric permittivity

PACS: 77.84.–s, 77.80.–e, 77.80.B– **DOI:** 10.1088/1674-1056/25/5/057704

1. Introduction

Chiral smectic liquid crystal product is organized in layers and has a helical structure. Because of the chirality and the molecular tilt with respect to the layer normal, the compound presents for some of its mesophases a ferroelectric character. The use of an SSFLC cell makes it possible to highlight this ferroelectric character.[1] During cooling, an increasing tilt angle θ is observed. One can also observe a subset of the following subphases: the SmA with $\theta = 0$; the SmC^*_α with $\theta \neq 0$ and an azimuthal angle Φ precessing with a short incommensurate period along the layer normal; the SmC^* with a long pitch helix and locally spontaneous polarization, and it is referred to be ferroelectric ($P_S \neq 0$; the SmC_{*Fi2} with a four-layers unit cell in which Φ has a non-regular increment ($\Delta\Phi \neq 2\pi/4$), a long pitch helix, and it has no macroscopic polarization ($P_S = 0$); the SmC^*_{Fi1} with a three-layers unit cell where Φ has a non-regular increment ($\Delta\Phi \neq 2\pi/3$), a long pitch helix, and it is polar phase with ($P_S \neq 0$); the SmC^*_A with a regular increment $\Delta\Phi = \pi$) within a two-layer unit cell, a long pitch helix and it is referred to be antiferroelectric ($P_S = 0$).[2–5]

In such compounds, the phase transitions can be induced as well by changing temperature by applying an electric field. A rise in the module of the applied field induces always a transition towards a SmC^* state where the helix is completely unwound.[6,7]

The applications of chiral smectic liquid crystals to several fields of technology imperatively require the knowledge of the field thresholds and the temperatures of the transitions. Consequently, a chart must be drawn in plan (E,T) in order to locate various domains of the phases and the lines which separate them. Several experimental methods are used to carry out this work, such as electro-optical method,[8,9] the dielectric spectroscopy method,[10–12] and finally the constant current method that was announced first by Marcerou.[13]

The complexity and the richness of the phase sequences of a chiral smectic liquid crystal support the appearance of several phenomena accompanying the phase transitions. Hysteresis phenomenon was observed each time and the optics or electric answers following an electric excitation were studied.[8,14,15] Metastable states were observed in mixtures[16] and recently a phenomenon of coexistence was highlighted.[17,18]

In this work we make a slight modification to the measurement principles based on the constant current method. This modification allows certain characteristic parameters of chiral smectic liquid crystals like the dielectric permittivity and the spontaneous polarization to be quantitatively measured. According to these new principles, measurements of these last parameters are conducted on two chiral smectic liquid crystal compounds belonging to a series of fluorinated compound CnF3 ($n = 10; 12$)[19,20] and on a reference product (MHPOBC[21]). A comparison of the measurements obtained by the constant current method with those obtained by the electro-optical one is carried out.[21,22]

Initially, we detail the principle of the constant current method. For that we introduce the thermodynamic considerations which lead to the development of this technique. A new rule of phase must be considered, making it possible to explain the appearance of coexistence of phases in the samples during a transition under electric field. Then we present the new measurement principles of the effective permittivity and the spontaneous polarization. With a square current signal, a

†Corresponding author. E-mail: hassen.dhaouadi@ipeit.rnu.tn

© 2016 Chinese Physical Society and IOP Publishing Ltd

ferroelectric hysteresis phenomenon is revealed. A remnant polarization, at null field, is observed.

2. Theoretical background

2.1. Mean-field theory of the para-ferroelectric phase transition

Before presenting the principle of the constant current method, we review the results of mean-field theory of the para-ferroelectric phase transition. Polarization P of the sample constitutes the order parameter of this transition. The Landau free energy is expressed according to P as

$$g = g_0 + \frac{1}{2}\alpha (T - T_c) P^2 + \frac{1}{4} b P^4. \tag{1}$$

Polarization P is null above T_c and elsewhere equal to

$$P = \sqrt{\frac{\alpha}{b}(T - T_c)}. \tag{2}$$

However, text books tell us that the quadratic term of this development must have the following expression:

$$\frac{1}{2}\alpha (T - T_c) P^2 = \frac{1}{2\varepsilon_0 \chi} P^2. \tag{3}$$

With an electric field applied, two other terms must be added in the development of Eq. (1) and by considering only the quadratic term, one obtains

$$g = g_0 + \frac{1}{2}\alpha (T - T_c) P^2 - \frac{1}{2}\varepsilon_0 \varepsilon E^2 - PE. \tag{4}$$

Minimization with respect to P gives the effective value of ferroelectric polarization

$$P_{\text{ferro}} = \varepsilon_0 \chi E = \frac{1}{\alpha (T - T_c)} E.$$

Since total polarization in the sample is

$$P = \varepsilon_0 \chi_\infty E + P_{\text{ferro}},$$

one finds

$$\varepsilon = 1 + \chi_\infty + \frac{1}{\varepsilon_0 \alpha (T - T_c)}, \tag{5}$$

where χ_∞ is the dielectric susceptibility which involves mainly electronic contributions.

One can notice easily that ε diverges at T_c. Then, to locate these phase transitions one can either measure polarization P according to the temperature (P vanishes at T_c) or observe the variation of the dielectric permittivity ε according to the temperature (ε shows divergence at T_c).

2.2. Method of constant current

The useful thermodynamic parameters of a system are in practice the pressure P, the volume V, the temperature T, and the entropy S. For studying the chiral smectic liquid crystals, one must consider two other parameters: the electric field E (intensive variable), with which one associates the electric excitation D (extensive variable brought back to the unit of volume). The qualitative description of a chiral smectic liquid crystal is thus made with the three intensive variables P, T, and E. The presence of these three intensive variables P, T, and E leads to changing of the rule of phase which gives the variance of the system ϑ,

$$\vartheta = C + 3 - \varphi, \tag{6}$$

where C is the number of components (1 for a pure substance) and φ is the number of phases. For a pure substance, the variance when two phases coexist is 2. The experiments on liquid crystals are generally carried out at a constant pressure. Then, as field-induced phase transitions generally hold true at a constant temperature, the value of the electric field is thermodynamically imposed.

If one crosses at constant temperature, in the (E, T) diagram, a curve separates two different phases of a chiral smectic liquid crystal and the two phases coexist if the transition is of first order ($\vartheta = 2$). As one works at constant temperature and pressure, one will have $\delta E = 0$. During the transition the electric field remains constant. This study constitutes the guiding principle of the constant current method that we will discuss in the following.

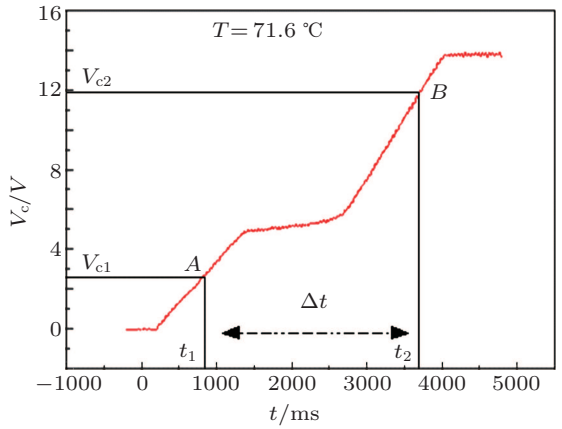


Fig. 1. (color online) Time dependence of V_c (constant current signal) for product C10F3 with a cell thickness of 5 μm and a constant current intensity of 5 nA. The slopes of the linear parts allow the values of ε_{eff} before and after the transition to be measured. The measurements of Δt and ΔV_c on both sides of a plateau make it possible to measure ΔP_s.

One deals with a phase transition between two tilted smectic phases with a different value of the polarization which are confined and aligned in the planar geometry in a capacitor of thickness e in order to apply an electric field parallel with the layer planes. If this capacitor is connected to a generator delivering a constant current of intensity $\boldsymbol{i}$ in a nanoampere range, the time dependence of the local electric field $\boldsymbol{E}$ in the cell which is given by measuring the capacitor voltage $E = V_c/e$ presents a linear growth at the beginning, followed by a plateau when the field threshold $\boldsymbol{E}_s$ is reached ($\boldsymbol{E}_s$ is the

value of field which induces a transition). The electric field is stabilized with this value until the complete disappearance of the ground phase (phase exists at weak fields). Afterwards, the increase begins again. Typical curves showing the evolution of the electric field in the cell with time reveal two types of answers with one or two plateaus according to the temperature at which we work (Fig. 1).

The values of slope τ of the linear parts of the curve depend on the static permittivity $\varepsilon_{\rm eff}$ as given below[13]

$$\varepsilon_{\rm eff} = \frac{i}{\varepsilon_0 \tau S}, \tag{7}$$

where S is the area of the plate of the capacitor and $\varepsilon_{\rm eff}$ is the effective permittivity that the compound has. $\varepsilon_{\rm eff}$ comprises of two contributions: the static permittivity $\varepsilon_\perp$ and a contribution due to the polarization of the sample following a possible distortion of the structure.

The width of the plateau Δt is directly related to the variation of spontaneous polarization $\Delta P_{\rm s}$ before and after the transition.

At any time, problems during measuring $\varepsilon_{\rm eff}$ and $\Delta P_{\rm s}$ are met. Indeed, because of the dependence of $\varepsilon_{\rm eff}$ on the electric field and the influence of a possible weak conduction of the cell in addition to surface effects, the linear parts become increasingly curved for increasing strong fields and it is not always possible to identify the beginning and the end of a plateau. Moreover, in the majority of cases, this plateau is not horizontal

Now, we present the principle of a measurement of $\varepsilon_{\rm eff}$ as well as a slight modification in the formula which allows the deduction of $\Delta P_{\rm s}$. The measurements of the slopes τ of the linear parts of the curves presented in Fig. 1 make it possible to deduce the sample permittivity values before and after a phase transition (Eq. (7)). If one considers the electric displacement D

$$D = \varepsilon_0 \varepsilon_{\rm eff} E + P_{\rm s}, \tag{8}$$

one can write the current in the circuit as

$$i = S\frac{\partial D}{\partial t}. \tag{9}$$

As the delivered current is constant, one has

$$\int_{t_1}^{t_2} i\,{\rm d}t = i\Delta t = S\Delta\left(\varepsilon_0 \varepsilon_{\rm eff} E + P_{\rm s}\right), \tag{10}$$

which gives

$$\Delta P_{\rm s} = \frac{i\Delta t}{S} - \varepsilon_0 \Delta\left(\varepsilon_{\rm eff} E\right). \tag{11}$$

Then for the measurement of $\Delta P_{\rm s}$, instead of the width of the plateau, one considers two unspecified points (A and B) belonging to the linear parts taken respectively before and after the transition (Fig. 1). A simple calculation makes it possible to express $\Delta P_{\rm s}$ according to Δt and $\Delta(\varepsilon_{\rm eff} E)$.

2.3. Use of periodic square current signal

To make an acceptable measurement of the permittivity in the unrolled SmC* phase, obtained at strong field, one uses a generator of current which delivers a periodic square signal of weak frequency. The answer that one obtains is a rectangular signal distorted by the plateaus corresponding to the phase transitions (Fig. 2). At the beginning of the rise period, the slope measured at this moment makes it possible to deduce the permittivity of the sample at strong field. For this case we must consider a slight correction of Eq. (7)

$$\varepsilon_{\rm eff} = \frac{i}{2\varepsilon_0 \tau S}. \tag{12}$$

Between two points A and B (Fig. 2), the polarization passes from the state up $(+P_{\rm S})$ to the state down $(-P_{\rm s})$ and $\Delta P_{\rm s} = 2P_{\rm s}$ ($P_{\rm S}$ is the ferroelectric polarization at saturation). The sample has in both cases the same dielectric permittivity, $\varepsilon_{\rm eff} = \varepsilon_\perp$. Then according to Eq. (11), one has

$$P_{\rm s} = \frac{|i|\,\Delta t}{2S} - \varepsilon_0 \varepsilon_{\rm eff} \frac{|\Delta V_{\rm c}|}{2e}, \tag{13}$$

where $|i|$ and $|\Delta V_{\rm c}|$ are respectively the absolute values of i and $\Delta V_{\rm c}$.

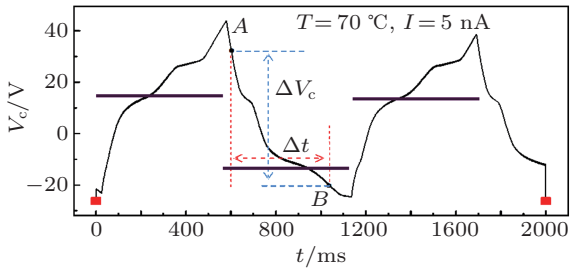


Fig. 2. (color online) Time dependence of cell voltage $V_{\rm c}$ (product C10F3 with a cell thickness of 5 μm and a current square signal of ±5 nA). The slope of the linear part at the beginning of the rise allows a measurement of $\varepsilon_{\rm eff}$ in the unrolled SmC* phase. The measurements of Δt and $\Delta V_{\rm c}$ on both unspecified points (A and B) make it possible to determine ΔP. Colored lines represent the square current signal.

3. Experiment

The liquid crystals studied were chiral smectic compounds named C10F3 and C12F3 belonging to the series of fluorinated products, CnF3 ($n = 10, 12$), synthesized by Essid *et al.*[19] and Manai.[20] For comparison, an experiment on a reference product (MHPOBC[21]) was carried out. The molecular structures of these compounds are shown in Fig. 3.

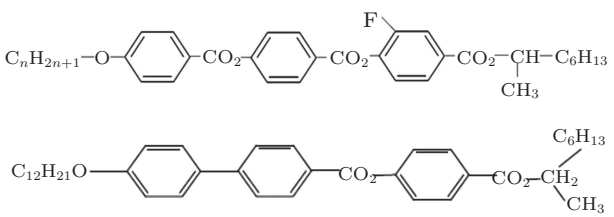


Fig. 3. Molecular structures of liquid crystals (CnF3), $n = 10, 12$; MHPOBC.

For these compounds, the zero field phase sequences are as follows:
For the product C10F3,

$$\mathrm{SmC^*_{Fi2}} \xrightarrow{64\ ^\circ\mathrm{C}} \mathrm{SmC^*_{\alpha}} \longrightarrow \mathrm{SmA} \longrightarrow \mathrm{Iso.}$$

For the product C12F3,

$$\mathrm{SmC^*_{Fi2}} \xrightarrow{67.2\ ^\circ\mathrm{C}} \mathrm{SmC^*} + \mathrm{SmC^*_{Fi1}} \longrightarrow \mathrm{SmC^*} \longrightarrow \mathrm{SmC^*_{\alpha}} \longrightarrow \mathrm{SmA} \longrightarrow \mathrm{Iso.}$$

For the product MHPOBC

$$\mathrm{SmC^*_A} \xrightarrow{117.2\ ^\circ\mathrm{C}} \mathrm{SmC^*_{Fi1}} \xrightarrow{118.2\ ^\circ\mathrm{C}} \mathrm{SmC^*_{Fi2}} \xrightarrow{119.2\ ^\circ\mathrm{C}} \mathrm{SmC^*} \xrightarrow{120.8\ ^\circ\mathrm{C}} \mathrm{SmC^*_{\alpha}} \xrightarrow{122\ ^\circ\mathrm{C}} \mathrm{SmA} \xrightarrow{150\ ^\circ\mathrm{C}} \mathrm{Iso.}$$

A polarizing microscope (Leitz Model Laborlux 12 Pols) was used to observe different liquid crystalline mesophases. Measurements were carried out on commercial cells (EHC, Japan) coated with a conductive layer of indium-tin oxide (ITO) and treated by polyvinyl alcohol (PVA) indirectly rubbed to ensure a planar alignment. The active area is 25 mm^2. At the isotropic phase, the liquid crystal was introduced by capillarity into the cell. The 5-μm and 8-μm cells were used for measurements. The sample cell was placed between crossed polarizers, with the smectic layer normal being parallel to one of the polarizers. The sample texture was automatically monitored with a digital camera mounted on the microscope. The temperature regulator was provided by a programmable DC power supply (HP E3632A), a programmable multimeter (Keithley Model 2000) and an oven developed in our laboratory. The temperature was controlled to be within ±0.01 °C.

A generator of current (Keithley 6200) delivers a constant current $\boldsymbol{i}$ of the order of the nano Ampere and voltage of the cell is controlled by an oscilloscope.

4. Results and discussion

4.1. Diagrams of constant current

Here we present some curves showing the evolutions of the cell voltage with time under a constant current, for product C10F with a cell thickness of 5 μm and $i = 5$ nA (Figs. 4(a) and 4(b)), product C12F3 with a cell thickness of 8 μm and $i = 10$ nA (Fig. 4(c)), and product MHPOB with a cell thickness of 5 μm and $i = 10$ nA (Fig. 4(d)). The curves presenting two plateaus (Figs. 4(a) and 4(c)) reveal the passage through an intermediate state between the phase null field, i.e., $\mathrm{SmC^*_{Fi2}}$, and the unrolled phase $\mathrm{SmC^*}$. The curves (Figs. 4(b) and 4(d)) present only one plateau corresponding to the transition $\mathrm{SmC_{\alpha}} \longrightarrow \mathrm{SmC^*}$ in both cases.

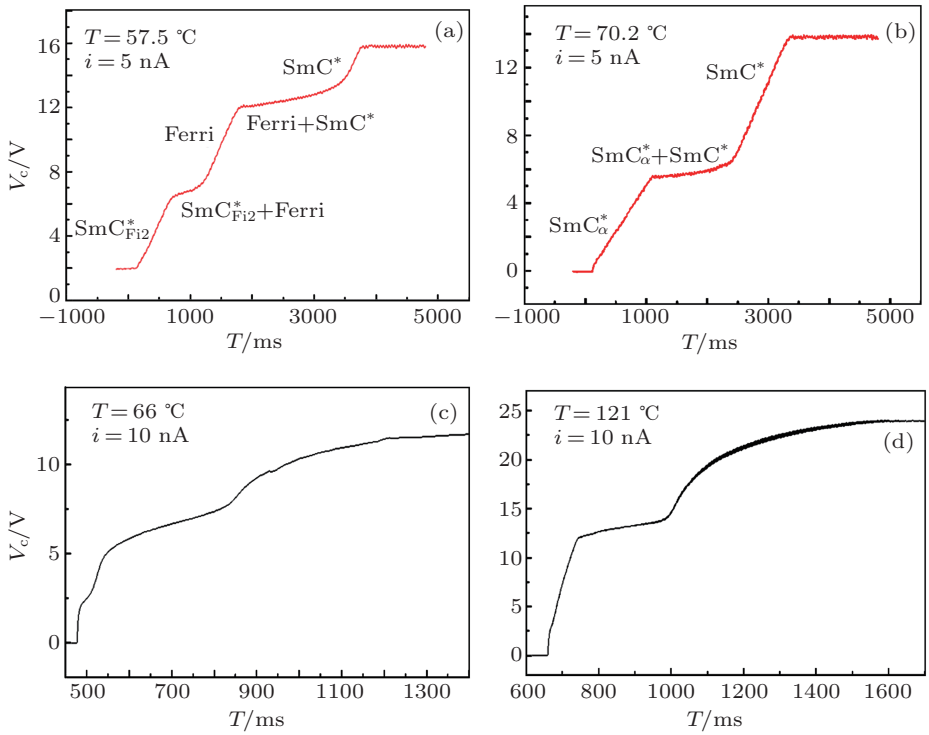


Fig. 4. (color online) Time dependences of cell voltage V_c (constant current signal) for (a) and (b) product C10F3 with a cell thickness of 5 μm and $i = 5$ nA, (c) product C12F3 with a cell thickness of 8 μm and $i = 10$ nA, and (d) product MHPOB with a cell thickness of 5 μm and $i = 10$ nA.

Monotonic increase at the initial phase with a slope being inversely proportional to the dielectric constant is due mainly to the charge of the capacitor. Plateaus correspond to the first order transitions. At these places the electric charges are used to compensate for the static polarization whose value changes. When the local field reaches its value $\boldsymbol{E} = \boldsymbol{E}_s$ at the cell

boundary, it is maintained as long as the second phase has not occupied the whole sample, with the two phases coexisting. Then the field increases again with a slope linked to the new dielectric constant.

For the compound C10F3, figures 4(a) and 4(b) show a typical behavior with quite linear parts and horizontal plateaus. Above the SmC_α phase (Fig. 4(a)) one observes only one plateau corresponding to the transition $SmC^*_\alpha \rightarrow$ unwounded SmC. The curve (Fig. 4(b)) presents two plateaus. It reveals the passage to an intermediate polar state so that one can allot the ferrielectric appellation to it.

Because of the weak conductivity in the cells, the linear parts become increasingly curved for increasing strong field. This is clearly observed in Figs. 4(c) and 4(d) for the compound (C12F3 and MHPOBC). From these figures it is not always possible to identify the beginning and the end of a plateau which makes it difficult to measure $\varepsilon_{\rm eff}$ and $\Delta P_{\rm s}$.

We need to record the evolution of the texture of the sample during a slow triangular variation of the cell voltage (Fig. 5). The passage towards the intermediate state is accompanied by a coexistence of two phases of different textures, which shows a true transition from the first order.

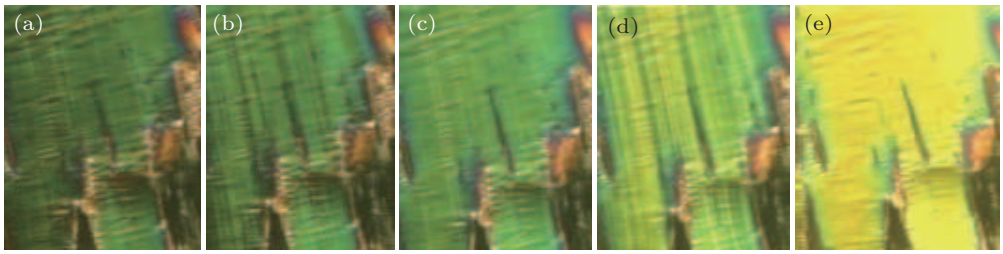


Fig. 5. (color online) Evolutions of the texture which have the C10F3 compound at temperature 60 °C, followed by a linear variation of the electric field, for (a) phase SmC^*_{Fi2}, (b) coexistent SmC^*_{Fi2} and ferrielectric phase, (c) ferrielectric phase, (d) coexistent ferrielectric and unrolled SmC^* phase, and (e) unrolled SmC^* phase.

The intermediate phase is the subject of a lot of research works to understand the origin and determine its structure. Jarad *et al.*[23] have measured the resonant x-ray diffraction and have shown that this phase is composed of three layers but the average orientation differs from that of common SmC^*_{Fi1} phase.

4.2. Measurements of $\varepsilon_{\rm eff}$ and $\Delta P_{\rm s}$

We present in Figs. 6(a)–6(c) some curves showing the evolution of the cell voltage with time under a square current signal. Figure 6(a) is for product C10F3 with a cell thickness of 5 μm and $i = 5$ nA, figure 6(b) for product C12F3 with a cell thickness of 8 μm and $i = 10$ nA and figure 6(c) for product MHPOB with a cell thickness of 5 μm and $i = 10$ nA.

The response of the sample to a periodic square current signal is a triangular signal distorted by the plateaus corresponding to the phase transitions. A delay with the transition between the rise part, corresponding to a positive current $+i_0$ and the descent one, corresponding to a negative current $-i_0$ are observed. Further, we will study this hysteresis phenomenon in more detail.

The curves of Fig. 7 represent the variations of the relative permittivity $\varepsilon_{\rm eff}$ with temperature for various phases of the product C10F3. To plot this curve we need to combine the experimental data of the two types of signals used. For measuring the values of $\varepsilon_{\rm eff}$ in the initial phase and the intermediate phase we use the experimental data in the case of constant current (Eq. (7)). For the measurement of $\varepsilon_{\rm eff}$ in the unrolled SmC^* phase, one uses the experimental results corresponding to the case of a square signal by considering the linear part at the beginning of the rise part (Eq. (12))

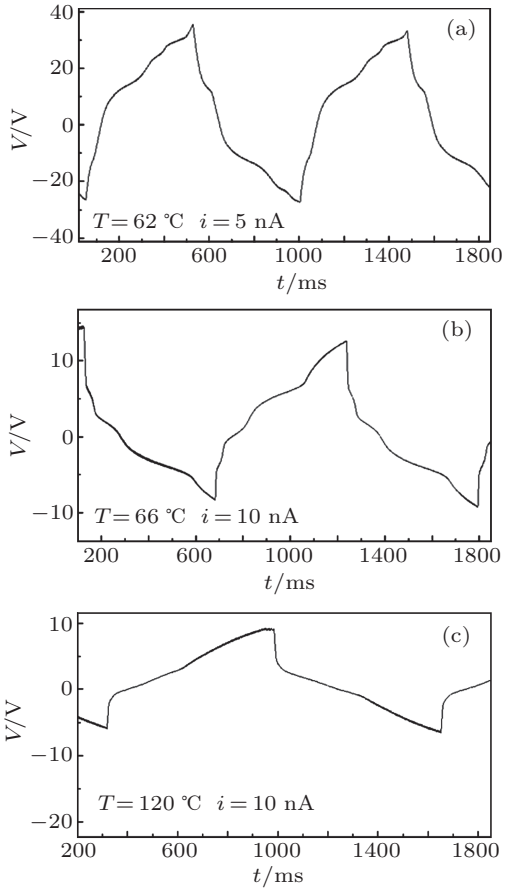


Fig. 6. Time dependences of cell voltage (square current signal). Panel (a) is for product C10F3 with a cell thickness of 5 μm and $i = 5$ nA, panel (b) for product C12F3 with a cell thickness of 8 μm and $i = 10$ nA and panel (c) for product MHPOB with a cell thickness of 5 μm and $i = 10$ nA.

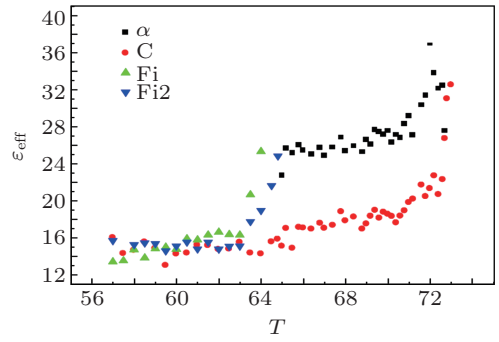


Fig. 7. (color online) Temperature dependences of the relative permittivity $\varepsilon_{\rm eff}$ (Product C10F3) for the SmC$_\alpha$ phase (black square), unwounded SmC* (red solid circle), SmC$^*_{\rm fi1}$ (green triangle) and SmC$^*_{\rm fi2}$ (blue inverted triangle). $\varepsilon_{\rm eff}$ increases quickly at the temperature of transition towards the SmA phase.

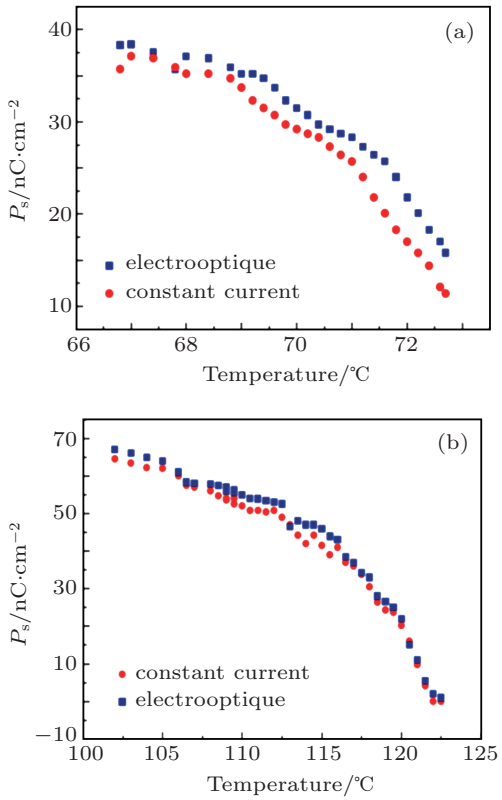


Fig. 8. (color online) Temperature dependences of the spontaneous polarization $P_{\rm S}$ for (a) product C10F3 and (b) product MHPOBC. Red solid circles represent the measurements by the method of constant current, and blue solid squares refer to the measurements by the electro-optical method.

As is well known, the susceptibility of the polarization P diverges at the second-order transition temperature (Eq. (5)). If one applies an external field at that time, the dipole will respond with large susceptibility and response time. In the system under study, the phase transitions seem to be of the first kind. But as often happens, one may expect to observe an enhancement of the susceptibility even if it is not of large divergence. One should also expect a great susceptibility at transition from a phase without polarization to a ferrielectric or ferroelectric one. Figure 7 clearly shows this phenomenon and various temperatures of the transitions under field can be foreseen. The value of the polarizations $P_{\rm s}$ in the ferroelectric SmC* phase, computed from Eq. (13), is compatible with the more accurate one obtained by conventional method. The experimental results obtained from the product C10F3 and MHPOBC (Figs. 8(a) and 8(b)) confirm the results obtained by the electro-optical method. The curves of spontaneous polarization according to the temperature take generally the envisaged forms given by Eq. (2).

4.3. Ferroelectric hysteresis

The response of the sample to a periodic square current signal points out that the cell voltage $V_{\rm c}$ is a triangular signal distorted by the plateaus corresponding to the phase transitions (Fig. 6). The two half periods of this answer are not symmetrical, which gives rise to a delay with the transition between the rising part, corresponding to a positive current $+i_0$ and the falling one, corresponding to a negative current, i_0. The number of observable transitions in each half period is the same one. The measurement of the variation of the polarization, computed from Eq. (13), gives almost the same values. This causes a reversibility of the transitions, i.e., the phases which appear in the rising part are the same as those in the falling part. Hence, a phenomenon of hysteresis appears. To highlight this phenomenon one carries out a cycle by making the beginning of the curve of rise coincide with the end of the curve of descent. The obtained cycles point out those hystereses of the ferroelectric products. Actually one traces the cycle in the (t, $V_{\rm c}$), where t is the time. The axis of $V_{\rm c}$ represents the electric field $\boldsymbol{E}$. The axis of time represents the electric excitation $\boldsymbol{D}$. Indeed, in the case of constant current i_0 we have

$$D = \frac{i_0 t}{S}. \tag{14}$$

Figure 9 shows the cycles for the product C10F3 at 62 °C, obtained by the method described previously. The axes were shifted and the scale of time is modified according to Eq. (14) in order to indicate the electric excitation $\boldsymbol{D}$.

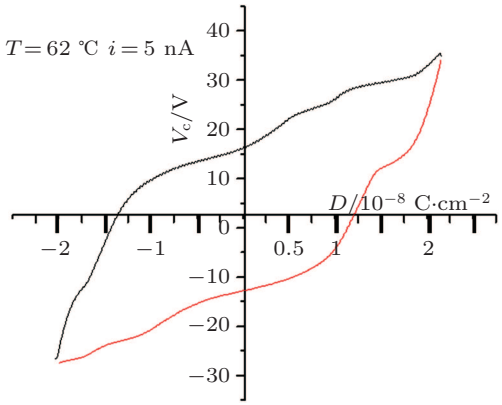


Fig. 9. (color online) Hysteresis loop obtained by current square signal $i_0 = 5$ nA for compound C10F3 at $T = 62$ °C.

All the observed cycles are characteristic of ferroelectric products with only one loop, which shows a phenomenon of

ferroelectric hysteresis, accompanied by the phase transitions. A remnant polarization at null field points out an effect of memory in these compounds.

5. Conclusion and perspectives

The constant current method allows the rapid determination of the (E,T) phase diagram of a given chiral smectic liquid crystal compound, but the weak precision of measurements reduces its utility. We improve the precision of measurements by adopting the new principles which give results comparable to those obtained by the traditional method.

Precisely measuring the spontaneous polarization and the dielectric permittivity can be a means of determining the natures or structures of phases.

The use of a square current signal shows reversibility in the appearance of the phases. The phases which appear in the rising part are the same as those which appear in the falling part, which means the stabilities of these phases obtained under field. A delay with the transition between the rising part and the falling part is observed, which highlights phenomena of ferroelectric hysteresis in these compounds.

All the transitions observed under field are first order, and both phases coexist in the sample all along the transition. The new rule of phase, introduced at the beginning, makes it possible to envisage such coexistence. Indeed, the variance calculated for a pure substance is equal to 2 where two phases coexist.

In conclusion, the improvements made in the principles of measurement of the characteristic parameters of a ferroelectric liquid crystal will make the constant current method a routine investigation method which allows relevant explanations of the structures and the nature of the phases.

References

[1] Meyer R B, Liebert L, Strzelecki L and Keller P 1975 *J. Phys. Lett.* **36** L69

[2] Chandani A D L, Gorecka E, Ouchi Y, Takezoe H and Fukuda A 1989 *Jpn. J. Appl. Phys.* **28** L1265

[3] Cady A, Pitney J A, Pindak R, Matkin L S, Watson S J, Gleeson H F, Cluzeau P, Barois P, Levelut A M and Caliebe W 2001 *Phys. Rev. E* **64** 050702

[4] Hirst L S, Watson S, Gleeson H F, Cluzeau P, Barois P, Pindak R, Pitney J, Cady A, Johnson P M and Huang C C 2002 *Phys. Rev. E* **65** 041705

[5] Olson D A, Han X F, Cady A and Huang C C 2002 *Phys. Rev. E* **66** 021702

[6] Lagerval S T 2004 *Ferrolectics* **301** 15

[7] Roy A and Madhusudana N V 1998 *Eur. Phys. Lett.* **41** 501

[8] Fukuda A, Takanichi Y, Isozaki T Ishikawa K and Takezoe H 1994 *J. Mater. Chem.* **4** 997

[9] Yu P, Panarin H, Xu S T, Maclughadha J K, Vij A, Seed M and Hird Goodby J W 1995 *J. Phys: Condens. Matter* **7** 351

[10] Dupont L, Glogarova M, Marcerou J P, Nguyen H T, Destrade C and Lecek L 1991 *J. Phys. II* **1** 831

[11] Sarmento S, Carvalho P S, Chaves M R and Pinto F 2001 *Liquid Crystals* **28** 679

[12] Sarmento S, Carvalho P S, Chaves M R and Pinto F 2001 *Liquid Crystals* **28** 1839

[13] Marcerou J P, Nguyen H T, Bitri N, Gharbi A, Essid S and Soltani T 2007 *Eur. Phys. J. E* **23** 319

[14] Aoki Y and Nohira H 1995 *Liquid Crystals* **19** 15

[15] Wu S L, Huang F K, Uang B J, Tsai W J and Liang J J 1995 *Liquid Crystals* **18** 715

[16] Kuczynski W and Goc F 2003 *Liquid Crystals* **30** 701

[17] Zgueb R, Dhaouadi H and Othman H 2014 *Liquid Crystals* **41** 1394

[18] Soltani T, Bitri N, Dhaouadi H, Gharbi A, Marcerou J P and Nguyen H T 2009 *Liquid Crystals* **36** 1329

[19] Essid S, Manai M, Gharbi A, Marcerou J P, Rouillon J C and Nguyen H T 2004 *Liq. Cryst.* **31** 1

[20] Manai M 2006 Etude des propriétés électriques et optiques de cristaux liquides présentant des phases smectiques chirales et les phases frustrées SmQ et L (Doctor Thesis)

[21] Shiji N, Chandani A D L, Nishiyama S, Oushi Y, Takezoe H and Fukuda A 1988 *Ferroelectrics* **85** 99

[22] Manai M, Gharbi A, Essid S, Achard M F, Marcerou J P, Nguyen H T and Rouillon J C 2006 *Ferroelectrics* **343** 27

[23] Jaradat S, Brimicombe P D, Osipov M A, Pindac R and Gleeson H F 2011 *App. Phys. Lett.* **98** 043501